

Minimally Intrusive SHM Systems Using Piezoelectric Nanofibers in Composite Laminates

FRANCESCO MONGIOI¹, TOMMASO TERNELLI¹,
TOMMASO MARIA BRUGO¹, FEDERICA ZONZINI²,
ROBERTO PALAZZETTI³, PAOLO BETTINI³,
LUCA DE MARCHI² and ANDREA ZUCHELLI¹

ABSTRACT

This work presents the development of a self-sensing Carbon Fiber Reinforced Polymer (CFRP) laminate embedding P(VDF-TrFE) nanofibers for real-time impact detection and localization. Four nanostructured sensors were embedded within the midplane of cross-ply laminates and compared against laminates incorporating commercial PZT sensors. A probabilistic impact localization algorithm based on Gaussian Process Regression and differential Time of Arrival (dToA) measurements were implemented. While PZT sensors exhibited higher localization accuracy (RMSE=2.32 cm) compared to nanofiber-based sensors (RMSE=3.37 cm), they caused more severe interfacial damage under low-velocity impacts. In contrast, the nanostructured sensors confined damage to the polymeric interlayer, preserving the CFRP integrity. The results highlight the potential of nanofiber-based sensing layers as a scalable, minimally invasive solution for Structural Health Monitoring in aerospace composites.

INTRODUCTION

The aerospace industry is undergoing a major shift from traditional metal alloys to carbon fiber-reinforced composites (CFRPs) in aircraft construction, aiming to improve performance and reduce weight in response to fuel costs and environmental regulations [1]. Although composites offer a high strength-to-weight ratio, they pose significant challenges in damage tolerance and detection. Unlike metals, which typically fail through fatigue cracking, composites may develop complex and barely visible damage such as delamination, which can critically reduce structural integrity [2].

¹Department of Industrial Engineering, University of Bologna, Viale Risorgimento 2, 40136, Bologna, Italy

²Department of Electrical, Electronic, and Information Engineering, University of Bologna, Viale Risorgimento 2, 40136 Bologna, Italy

³Politecnico di Milano, via La Masa 1 – 20156 – Milan, Italy

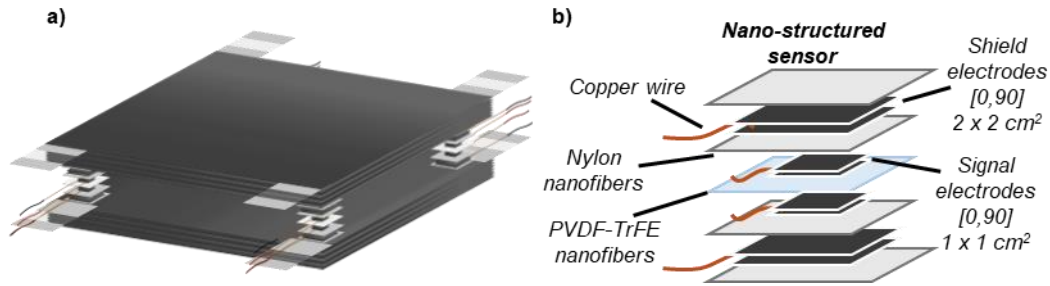


Figure 1 cross ply CFRP lamiate sensorized with 4 nanostructured sensors placed at the midplane on the plate verteces a). Nano-structured CFRP sensors based on PVDF-TrFE nanofibers b)

Structural Health Monitoring (SHM) systems have emerged as an effective solution for in-service damage detection. While conventional Non-Destructive Evaluation (NDE) techniques (e.g., ultrasonics, radiography) require aircraft downtime, SHM systems allow real-time monitoring with minimal operational disruption. These systems often use surface-mounted or embedded sensors; however, the former are prone to environmental degradation, while the latter may degrade the laminate's mechanical performance [3], [4].

Piezoelectric ceramics like Lead Zirconate Titanate (PZT) are commonly used for impact detection due to their high sensitivity to elastic waves [5], though their brittleness makes them susceptible to cracking. Alternatives such as Fiber Bragg Gratings also introduce stress concentrations [6]. Piezoelectric polymers like poly(vinylidene fluoride–trifluoroethylene) (P(VDF-TrFE)) offer greater mechanical flexibility and can be integrated within laminates to monitor damage evolution.

This study presents a preliminary investigation on embedding electrospun P(VDF-TrFE) nanofibers into CFRP laminates to enable self-sensing capabilities. Carbon fibers serve as in-situ electrodes, allowing the detection of elastic waves generated by impact events. Using Acoustic Emission (AE) monitoring and probabilistic localization algorithms based on Gaussian Processes (GPs), the system estimates the impact location through differential Time of Arrival (dT_{oA}) analysis. This approach enables real-time, minimally invasive damage localization, offering a scalable and structurally compatible solution for SHM in aerospace composites.

MATERIALS & METHODS

Fabrication of the Self-Sensing Plate

A cross-ply CFRP laminate with a stacking sequence of $[(0^\circ, 90^\circ)_2]_s$ was fabricated using T700 unidirectional prepreg (170 g/m², AvioUD170). Four nanostructured sensors were embedded at the plate corners (250 × 250 mm), positioned at the midplane (Figure 1a).

The sensor stacking sequence was $[(\text{CFRP-}90^\circ)/(\text{CFRP-}0^\circ)/N_{\text{ynf}}/(\text{CFRP-}90^\circ)/(\text{CFRP-}0^\circ)/\text{P}(\text{VDF-TrFE})_{\text{nf}}]_s$, as shown in Figure 1b. All the CFRP plies of the sensor were made from unidirectional prepreg (50 g/m², Reglass H.T. S.r.l.). A Nylon-6,6 nanofiber layer electrically insulated the sensor from the surrounding laminate. Outer CFRP plies (20 × 20 mm) acted as shielding electrodes to suppress triboelectric noise, while intermediate Nylon-6,6 membranes (10 × 10 mm) insulated them from the

signal electrodes. At the core, the P(VDF-TrFE) nanofibrous mat served as a charge generator.

Nanofiber mats fabrication

The piezoelectric nanofibrous mat was fabricated starting from a polymeric solution prepared by dissolving 20 wt% of the copolymer P(VDF-TrFE) (70/30 mol%, $M_w = 200$ kDa; kindly provided by Solvay S.p.A., Milan, Italy; <https://www.solvay.com>) in a solvent mixture of dimethylformamide (DMF, 45 wt%) and acetone (55 wt%). The resulting solution was electrospun using a four-needle drum collector electrospinning apparatus (Lab Unit, Spinbow®). A high voltage of 20.5 kV was applied to the needles, and the nanofibers were collected on a rotating drum (tangential speed: 0.4 m/s) placed 18 cm from the needles and electrically grounded. Electrospinning was performed at a flow rate of 0.75 mL/h per needle under controlled environmental conditions (22 °C, 55% relative humidity).

The insulating Nylon-6,6 nanofibers were produced by dissolving 16 wt% of Nylon-6,6 (Zytel E53NC010, DuPont) in a 1:1 v/v mixture of formic acid and chloroform. The electrospinning process was carried out in the same electrospinning machine by applying 27 kV to the high-voltage needles, with fibers collected on a grounded drum rotating at a tangential speed of 0.4 m/s. The needle-to-collector distance was set to 13 cm, and the polymer solution was fed at a rate of 0.4 mL/h per needle. Temperature and relative humidity were maintained at 20 °C and 35%, respectively.

By correctly setting the process duration of electrospinning, two mats were produced for P(VDF-TrFE) and for Nylon respectively, with useful thicknesses of 230 μm for P(VDF-TrFE) and 140 μm for Nylon.

Curing and Poling Process for the Sensorized Plate

The self-sensing plate was cured in an autoclave under a vacuum bag pressure of -950 mbar and external pressure of 6 bar. The cycle included a 30-minute dwell at 50 °C, followed by 4 hours at 100 °C with 1 °C/min heating ramps. The initial stage reduced epoxy viscosity to enhance nanofiber impregnation without triggering cross-linking. The second ensured full matrix curing ($T_g = 120$ °C) without exceeding the melting temperatures of Nylon-6,6 and P(VDF-TrFE) nanofibers (270 °C and 145 °C), preserving their structure.

The piezoelectric response of P(VDF-TrFE) stems from its β -phase crystalline structure. While electrospinning promotes β -phase formation, poling is required to align ferroelectric dipoles and induce macroscale piezoelectricity. In epoxy-embedded nanofibers, electric field distribution is non-uniform due to differences in permittivity and volume fraction [7], [8].

Poling was carried out by applying a 5 kV/mm electric field for 10 minutes at 100 °C, near the polymer's Curie temperature ($T_c = 103$ °C), using four generators (Keithley Model 248). Electrodes were grounded for 24 hours after the poling process to eliminate residual charges and ensure stable signal output.

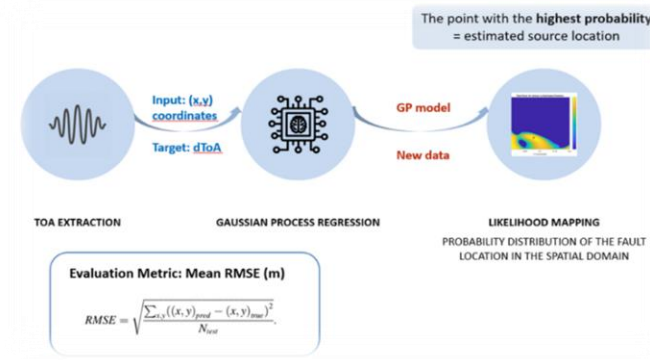


Figure 2 Impact localization algorithm flowchart

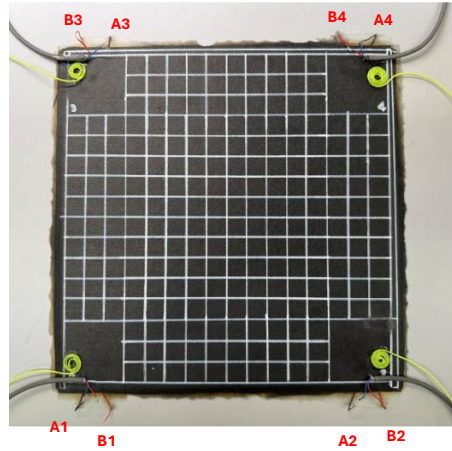


Figure 3 Sensorized composite plate with the impact grid layout

Electromechanical Characterization

The effective piezoelectric strain coefficient d_{33}^{eff} of the P(VDF-TrFE)/epoxy interlayer was then determined following the method described in [9], using the relation:

$$d_{33}^{eff} = S * C \quad (1)$$

where C is the capacitance measured between the signal electrodes, using an RLC meter (GW-Instek 6002), and S is the sensor sensitivity (mV/kN). Sensitivity was obtained by applying a sinusoidal compressive load (0.6–1.1 kN, 20 Hz) using an Instron 8033 testing machine. The voltage output from the sensor was recorded using an INA118-amplifier, and S was computed as the ratio of the peak-to-peak voltage to the peak-to-peak force.

Impact Localization Method

The impact localization algorithm used in this study follows the methodology proposed by Jones et al. [10], and is schematically illustrated in Figure 2. It combines two main techniques:

1. Akaike Information Criterion (AIC) for estimating the Time of Arrival (ToA) of the Acoustic Emission (AE) signal at each sensor.

2. Gaussian Process Regression (GPR) is employed to map impact source coordinates to expected dToA values across sensor pairs.

Signals from embedded sensors are initially processed using a band-pass filter, with cutoff frequencies selected through Power Spectral Density (PSD) analysis to isolate impact-relevant components. ToA values are estimated using the AIC method, and the resulting dToAs are used as inputs to the GPR model. Localization is performed via the Likelihood of Emission Location (LoEL) approach which evaluates the similarity between observed dToAs and the model-predicted values for each point on the plate, generating a spatial likelihood map. The predicted coordinates $(x, y)_{pred}$ are compared with the actual coordinates $(x, y)_{true}$ and localization accuracy is quantified using the Root Mean Square Error (RMSE).

The model was trained on a grid of 100 impact points (Figure 3), generated by dropping a 7 g steel sphere from 21 cm. 80% of the data was used for training, while 20% was reserved for validation.

Low velocity impact tests

Low-velocity impact tests (LVI) tests were conducted on three different types of laminate: a reference laminate, a laminate sensed with commercial PZT sensors, and finally one sensorized with piezoelectric nanofibers, to investigate the effect of the commercial PZT sensors and the nanofibers interleaving on the impact strength. The tests were conducted following the ASTM D7136 standard [11], using a drop-weight machine with a 1.3 kg impactor mass equipped with a PCB 208C05 load cell and 12.7 mm hemispherical steel tip. To adapt to the small dimensions of the laminates, the specimens were leaned on a support plate with a cylindrical hole with a diameter of 20 mm. A laser device was used to monitor the pre- and post-impact velocity of the impactor. Both the laser device and load cell signals were simultaneously acquired at 100 kHz. All the laminate types were impacted at an energy level equal to 3 J.

RESULTS & DISCUSSIONS

Electromechanical Performances

From a self-sensing perspective, the laminate was characterized in terms of sensitivity, and effective piezoelectric coefficient (d_{33}^{eff}). The output voltage and the applied load as a function of time are shown in Figure 4. The measured sensitivity was found to be 3.6 V/kN in the unshielded configuration [9]. However, for real-world applications, shielding electrodes are necessary to mitigate triboelectric noise and electromagnetic interference. To evaluate the d_{33}^{eff} of the piezoelectrically active interlayer, the measured sensitivity was multiplied by the capacitance evaluated between the piezo active interlayer (C), as described in Ref. [12]. Given that the C was measured to be 110 pF, the resulting d_{33}^{eff} was calculated to be 0.4 pC/N.

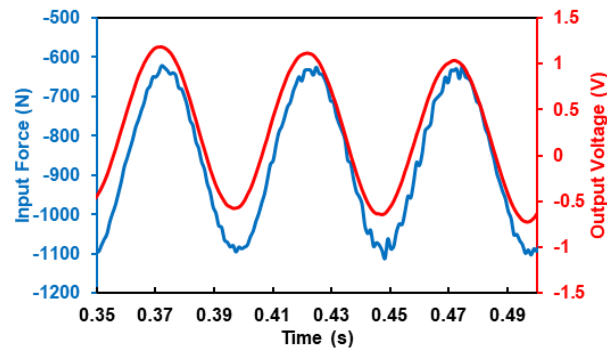


Figure 4 Piezoelectric voltage during compressive cyclic load

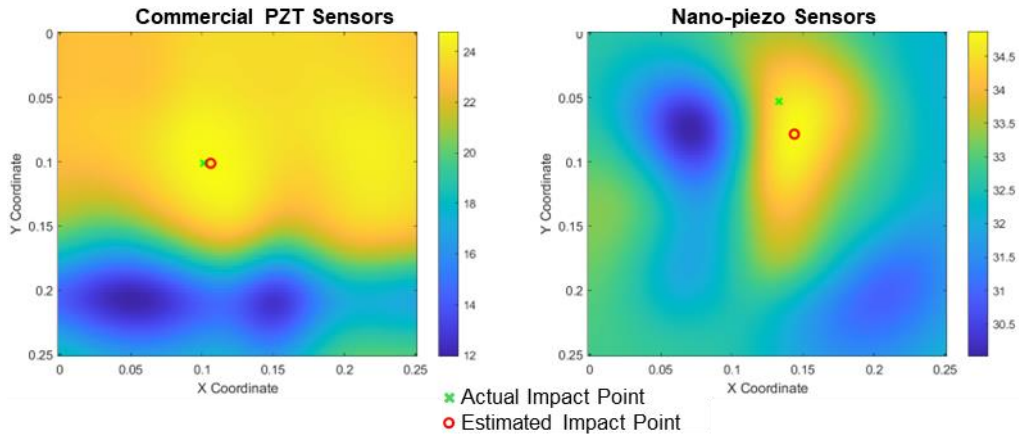


Figure 5 Likelihood maps showing the probability distribution of the impact location for the plate with PZT sensors (left) and Nano-piezo sensors (right).

Impact Location Estimation

Figure 5 shows the likelihood maps generated by comparing AE signals from impact events with those predicted by the Gaussian Process model. The plate with commercial PZT sensors demonstrates superior localization accuracy, with an RMSE of 2.32 cm compared to 3.37 cm for the nanofiber-based sensors.

This performance gap is mainly due to the higher sensitivity and signal-to-noise ratio (SNR) of the commercial sensors, which improves the accuracy of ToA estimation using the Akaike Information Criterion (AIC).

In both cases, however, the likelihood maps show a wide spatial distribution, suggesting that AIC-based ToA estimation may be suboptimal for composite laminates, where anisotropy introduces complex, direction-dependent wave propagation.

Low Velocity Impacts & Micrographs

As shown in Figure 6, the stiffnesses of the three laminates are comparable, as indicated by the overlapping initial slopes of their load–time curves. A force drop between 2.5 and 3 kN suggests the onset of damage such as fiber breakage or delamination. Notably, the laminate with commercial PZT sensors exhibits this drop earlier, while the one with nanofibrous sensors shows a higher maximum force than the reference, likely due to the added toughness of the nanofibrous interlayer. The reference laminate also displays greater maximum displacement, indicating more extensive damage and reduced stiffness.

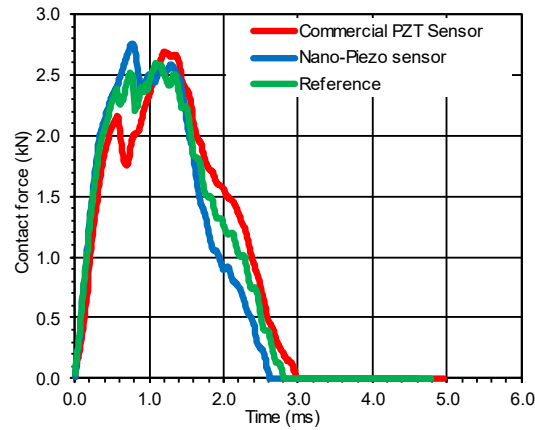


Figure 6 Contact force vs time of the laminates interleaved with the nanofibrous sensor (blue), commercial PZT sensor (red), and the reference laminate (green)

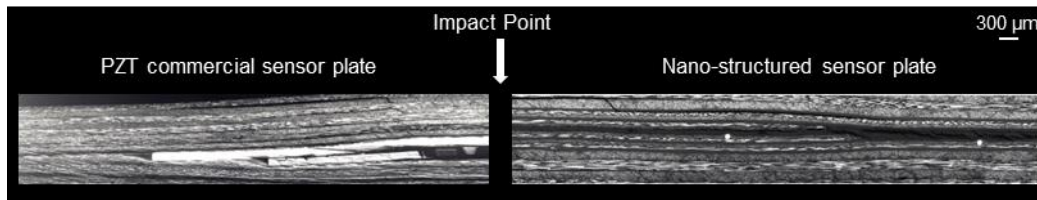


Figure 7 Micrographs analyses of the cross-section of the PZT commercial sensor plate and the Nano-structured sensor plate, after the LVI tests.

Figure 7 compares cross-sectional micrographs of the impacted laminates. In the PZT-sensor plate, brittle fracture of the ceramic disk is evident, causing delamination at the sensor-composite interface due to mechanical property mismatch. In contrast, delamination in the nanofiber-sensor plate is confined to the upper layers, with shear failure occurring within the nanofibrous interlayer itself, attributed to its lower mechanical properties.

While the thick nanofibrous interlayer may slightly reduce mechanical performance, it enhances toughness, limiting crack propagation and plastic deformation. This helps preserve the integrity of the CFRP layers, which are critical for load bearing. Preserving the integrity of the CFRP layers is crucial, as damage to the carbon fibers would compromise the mechanical performance and structural reliability of the component.

CONCLUSIONS

A self-sensing CFRP laminate embedding electrospun P(VDF-TrFE) nanofibers was developed and compared against a configuration with commercial PZT sensors. While PZT-equipped plates achieved better impact localization accuracy (RMSE = 2.32 cm vs 3.37 cm), they induced more severe interfacial damage under impact. In contrast, the nanofiber-based sensors preserved the mechanical integrity of the CFRP laminate by confining damage within the nanofibrous interlayer. Although the nanostructured sensors exhibited lower signal-to-noise ratios, they demonstrated consistent self-sensing capability with minimal structural impact. These findings suggest that nanofiber-based

sensors represent a promising strategy for integrating scalable, minimally invasive Structural Health Monitoring (SHM) functionalities into aerospace composites.

ACKNOWLEDGEMENTS

This research was funded by PRIN 2022 PNRR SELF-RE-PREG: Self-Sensing Interleaving for Recycled Prepreg (CUP: J53D23015920001), by European Union NextGenerationEU - National Sustainable Mobility Center (CN00000023) Spoke 11 - Innovative Materials & Light-weighting, by the Project Ecosyster - Ecosystem for Sustainable Transition in Emilia-Romagna (CUP J33C22001240001), and by CYPHER Project (CUP: E37G22000470007) and PRIN 2022 Project 3DSHYMCO (CUP: J53D23002470006). The authors would like to thank Solvay and Alessio Marrani for providing the polymers and BA student Johanna Quack and the M.Eng. student Riccardo Artioli for contributing in the development of the self-sensing sensing plate

REFERENCES

- [1] V. Giurgiutiu, "Introduction," in *Structural Health Monitoring of Aerospace Composites*, Elsevier, 2016, pp. 1–23. doi: 10.1016/b978-0-12-409605-9.00001-5.
- [2] C. H. Wang, "Progressive multi-scale modelling of composite laminates," in *Multi-Scale Modelling of Composite Material Systems: The Art of Predictive Damage Modelling*, Elsevier, 2005, pp. 259–277. doi: 10.1533/9781845690847.259.
- [3] X. Zeng, B. Zhao, X. Liu, Y. Yu, J. Guo, and X. Qing, "Lamb wave-based damage assessment for CFRP composite structures using a CHMM-based damage localization algorithm and a damage quantitative expression," *Mech. Syst. Signal Process.*, vol. 184, no. April 2022, p. 109750, 2023, doi: 10.1016/j.ymsp.2022.109750.
- [4] H. T. Oh, J. I. Won, S. C. Woo, and T. W. Kim, "Determination of impact damage in cfrp via pvdf signal analysis with support vector machine," *Materials (Basel)*, vol. 13, no. 22, pp. 1–23, 2020, doi: 10.3390/ma13225207.
- [5] S. Masmoudi, A. El Mahi, and S. Turki, "Use of piezoelectric as acoustic emission sensor for in situ monitoring of composite structures," *Compos. Part B Eng.*, vol. 80, pp. 307–320, 2015, doi: 10.1016/j.compositesb.2015.06.003.
- [6] M. Gabardi *et al.*, "Embedding Fiber Bragg Grating Sensors in Carbon Composite Structures for Accurate Strain Measurement," *IEEE Sens. J.*, vol. 23, no. 15, pp. 16882–16892, 2023, doi: 10.1109/JSEN.2023.3285408.
- [7] M. E. Gino *et al.*, "On the design of a piezoelectric self-sensing smart composite laminate," *Mater. Des.*, vol. 219, p. 110783, 2022, doi: 10.1016/j.matdes.2022.110783.
- [8] G. Selleri *et al.*, "Self-sensing composite material based on piezoelectric nanofibers," *Mater. Des.*, vol. 219, p. 110787, 2022, doi: 10.1016/j.matdes.2022.110787.
- [9] F. Mongioli, G. Selleri, E. Maccaferri, D. Fabiani, A. Zucchelli, and T. M. Brugo, "CFRP laminate with autonomous sensing and enhanced impact resistance by P(VDF-TrFE) nanofibers interleaving," *Compos. Part B Eng.*, vol. 293, no. June 2024, p. 112143, 2025, doi: 10.1016/j.compositesb.2025.112143.
- [10] M. R. Jones, T. J. Rogers, K. Worden, and E. J. Cross, "A Bayesian methodology for localising acoustic emission sources in complex structures," *Mech. Syst. Signal Process.*, vol. 163, p. 108143, Jan. 2022, doi: 10.1016/J.YMSSP.2021.108143.
- [11] ASTM D7136, "Standard test method for measuring the damage resistance of a fiber-reinforced polymer matrix composite to a drop-weight impact event," 2012. doi: 10.1520/D7136.
- [12] T. M. Brugo *et al.*, "Self-sensing hybrid composite laminate by piezoelectric nanofibers interleaving," *Compos. Part B Eng.*, vol. 212, no. February, p. 108673, 2021, doi: 10.1016/j.compositesb.2021.108673.